BIOCHEMISTRY
including biophysical chemistry & molecular biology

ARTICLE

pubs.acs.org/biochemistry

# Contribution of Active Site Residues to Substrate Hydrolysis by USP2: Insights into Catalysis by Ubiquitin Specific Proteases†

Wanfang Zhang,[‡] Traian Sulea,[§] Limei Tao,[§] Qizhi Cui,[§] Enrico O. Purisima,[§] Ratsavarinh Vongsamphanh,[§] Paule Lachance,[§] Viktoria Lytvyn,[§] Hongtao Qi,[§] Yuxin Li,[*,‡] and Robert Ménard[*,§]

[‡]Institute of Genetics and Cytology, Northeast Normal University, Changchun 130024, People's Republic of China

[§]Biotechnology Research Institute, National Research Council of Canada, Montréal, Québec, Canada H4P 2R2

Supporting Information

**ABSTRACT:** The ubiquitin-specific protease (USP) structural class represents the largest and most diverse family of deubiquitinating enzymes (DUBs). Many USPs assume important biological roles and emerge as potential targets for therapeutic intervention. A clear understanding of USP catalytic mechanism requires a functional evaluation of the proposed key active site residues. Crystallographic data of ubiquitin aldehyde adducts of USP catalytic cores provided structural details on the catalytic triad residues, namely the conserved Cys and His, and a variable putative third residue, and inferred indirect structural roles for two other conserved residues (Asn and Asp), in stabilizing via a bridging water molecule the oxyanion of the tetrahedral intermediate (TI). We have expressed the catalytic domain of USP2 and probed by site-directed mutagenesis the role of these active site residues in the hydrolysis of peptide and isopeptide substrates, including a synthetic K48-linked diubiquitin substrate for which a label-free, mass spectrometry based assay has been developed to monitor cleavage. Hydrolysis of ubiquitin-AMC, a model substrate, was not affected by the mutations. Molecular dynamics simulations of USP2, free and complexed with the TI of a bona fide isopeptide substrate, were carried out. We found that Asn271 is structurally poised to directly stabilize the oxyanion developed in the acylation step, while being structurally supported by the adjacent absolutely conserved Asp575. Mutagenesis data functionally confirmed this structural role independent of the nature (isopeptide vs peptide) of the bond being cleaved. We also found that Asn574, structurally located as the third member of the catalytic triad, does not fulfill this role functionally. A dual supporting role is inferred from double-point mutation and structural data for the absolutely conserved residue Asp575, in oxyanion hole formation, and in maintaining the correct alignment and protonation of His557 for catalytic competency.

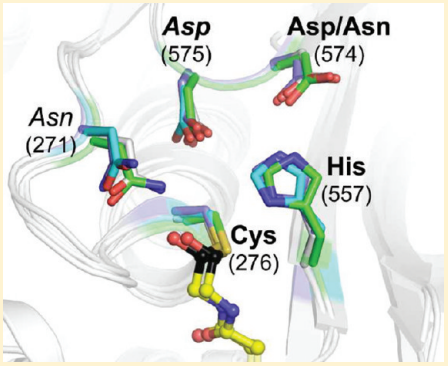


Protein ubiquitination is a post-translational modification that regulates a wide variety of cellular processes by affecting the stability, localization, and/or function of the modified proteins.[1−3] Conjugation of ubiquitin to target proteins is accomplished via a complex but relatively well-understood mechanism that involves the sequential action of three classes of enzymes: E1 (ubiquitin activating enzyme), E2 (ubiquitin conjugating enzyme), and E3 (ubiquitin protein ligase), which activate and transfer ubiquitin (Ub) or ubiquitin-like (Ubl) modifiers to the ε-amino group of an internal lysine residue of target proteins.[4−6] Attachment of Lys48-linked polyubiquitin chains promotes protein degradation by the Ub−proteasome system,[7] while non-proteasomal functions of Ub involve the attachment of differently linked polyubiquitin chains and individual Ub molecules.[8−10]

Ubiquitination is a reversible process. The isopeptide bond that links the C-terminal glycine of ubiquitin to a lysine side chain on the target protein, or on another ubiquitin molecule in a polyubiquitin chain, can be cleaved by deubiquitinating enzymes (DUBs).[11−14] These enzymes are also responsible for the activation of ubiquitin and ubiquitin-like modifiers by C-terminal processing of their precursors. Approximately 100 putative mammalian DUBs have been identified in the human genome, which can be grouped into five different families, four of which are cysteine proteases: the ubiquitin-C-terminal hydrolases (UCHs, MEROPS family C12),[15] ubiquitin-specific proteases (USPs, families C19, C16, C67), ovarian-tumor (OTU) domain-containing enzymes (otubains, families C64, C65), and the Machado-Joseph domain (MJD, family C86) DUBs.[12−14]

The ubiquitin-specific protease (USP) structural class represents the largest and most diverse family of DUBs, with over 50 members in humans. Although the precise in vivo functions of several DUBs remain unclear, important biological roles have been discovered recently for many members of this family.[14,16,17] Often, this was accomplished by determining their protein interacting partners, which can act as substrates or activity modulators.[16] In addition, several pathological conditions have

**Received:** December 8, 2010
**Revised:** March 18, 2011
**Published:** May 04, 2011

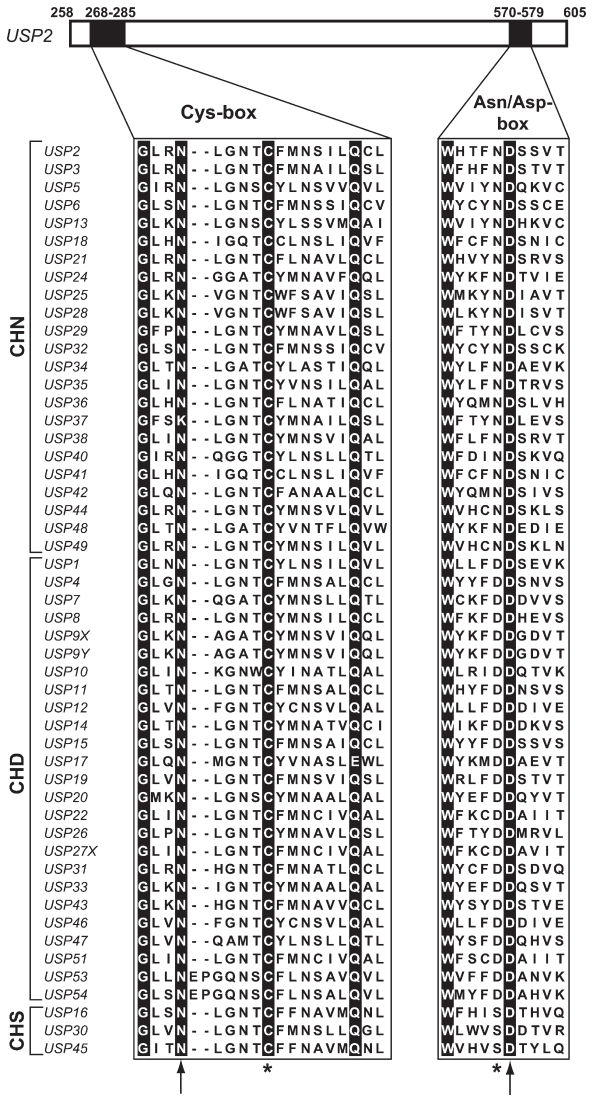


**Figure 1.** Multiple sequence alignment of catalytic cores of human USPs. Black shading represents positions with >95% conservation. Inactive USPs 39, 52 (lacking active site Cys and His residues), and 50 (with a C-terminally truncated core domain) are not included. Residues involved in the catalytic triad are marked with an asterisk, and those putatively involved in oxyanion stabilization are indicated by arrows. USPs are grouped according to their catalytic triads into three classes: CHN (cysteine−histidine−asparagine), CHD (cysteine−histidine−aspartate), and CHS (cysteine−histidine−serine). Not shown: His557, conserved in 51 of 54 USPs.

been linked to USP dysfunction, such as cancer and neurological disease,[17−20] and these enzymes represent an emerging class of potential targets for therapeutic intervention.

USPs have a catalytic core domain of ∼350 amino acids, which possesses the conserved catalytic triad signature of cysteine proteases, namely a cysteine, a histidine, and a third residue, most often Asp or Asn. For several of them, highly variable sequences upstream, downstream, and/or inserted within the catalytic domain are also found, representing potential or confirmed additional protein interaction domains. The determination of the structure of USP7, both free and complexed with a ubiquitin aldehyde inhibitor (Ubal), provided the first view of the overall architecture of the catalytic domain for this class of enzymes.[21] The structure showed that USP7 adopts a papain-like fold, with an additional extended, fingers-like domain which forms the ubiquitin binding pocket, and allowed to confirm the identities of the catalytic triad Cys223-His464-Asp481 residues. Interestingly, these residues were found to be misaligned in the unliganded structure, which lead to the proposal of a conformational change following Ub substrate binding leading to the catalytically competent form of the enzyme.

Additional USP structures solved indicate that despite low sequence similarity, the USP domain architecture is highly conserved.[22−24] The structure of USP2[a], solved only in liganded form in presence of Ubal or ubiquitin, possesses a similar organization of catalytic triad residues as that found in USP7, with the exception that the third member of the triad is an Asn instead of the Asp found in USP7.[24] Notably, the Cys276-His557-Asn574 arrangement of USP2 is found in approximately half of the human USP sequences (Figure 1), and the structure of USP2 is the only one available for this subgroup of human enzymes (the structure of yeast Ubp6, with the same catalytic triad of residues, has also been determined). For three USPs (USP16, USP30, and USP45), a serine residue is found instead of Asp/Asn as the third member of the triad. It has been reported that USP16 and USP30 retain enzymatic activity against a model substrate,[13] raising questions regarding the role played by the third member of the catalytic triad of USPs. The oxyanion hole residues, Asn271 and Asp275 (which structurally supports the former) in USP2, are both conserved in all human USP sequences (except Asn271 being a Lys in USP37) (Figure 1). This Asn/Asp tandem is poised to stabilize the oxyanion reaction intermediate formed during substrate hydrolysis.[21] However, in both USP2-Ubal (PDB code 2IBI) and USP7-Ubal (PDB code 1NBF) crystal structures, a water molecule appears to bridge both the putative oxyanion hole residues to the oxygen atom of the formed thiohemiacetal, and only indirect specific interactions with these residues were proposed.

A clear understanding of DUB catalytic mechanism requires an evaluation of the proposed functional contributions of key active site residues to catalysis. Limited information on this subject can be found in the literature. Site-directed mutagenesis performed on USP7 demonstrated the importance of several residues for substrate recognition and/or catalysis.[21] Using an in vitro assay for cleavage of Lys48-linked diubiquitin, it was shown that mutation to Ala of each of the three catalytic triad and two oxyanion hole residues, as well as residues in contact with the substrate in USP7, resulted in undetectable levels of activity in the gel-based assay. However, the variability in the nature of the third catalytic triad residue in USPs, which is also observed for the OTU family of DUBs, raises similar issues regarding the identity, and conservation of the catalytic triad,[12] and the presence of a water molecule interacting with the reaction intermediate modeled from the Ubal complexes, warrants further investigations of the structural and functional roles of these active site residues. For this purpose, we have expressed the catalytic domain of USP2 and used site-directed mutagenesis to probe the role of active site residues in the hydrolysis of peptide and isopeptide substrates. In addition, molecular dynamics simulations of USP2, free and complexed as a tetrahedral intermediate with a bona fide isopeptide substrate, were used to shed light into the oxyanion-stabilizing network in USPs.

We found that Asn271 is structurally poised to directly stabilize the oxyanion developed in the acylation step of the hydrolysis, being supported by hydrogen bonding with the adjacent Asp575, which is absolutely conserved in the USP family. Mutagenesis data confirm this structural role for hydrolysis of Ub substrates, independent of the nature (isopeptide vs peptide) of the bond being cleaved.

Hydrolysis of ubiquitin-AMC, however, is not affected by mutation of these two oxyanion hole residues alone or in combination, possibly due to the faster kinetics with the AMC substrate leading to a deacylation rate-limiting step, whereas the oxyanion hole stabilization is manifested mostly in the acylation step. We also find that Asn574, structurally located as the third member of the catalytic triad, does not fulfill this role functionally. A dual supporting role is inferred from double-point mutation data for the absolutely conserved residue Asp575, in oxyanion hole formation, and in maintaining the correct alignment and protonation of His557 for catalytic competency.

## MATERIALS AND METHODS

**Generation of USP2 Mutants.** The catalytic domain of human USP2 (residues 258−605) was amplified by PCR using cDNA purchased from Open Biosystems (Hunstville, AL; clone ID #3543435; accession# BC002955) and primers OVL191F (5′ACAACTAGTAATAATTTTGTTTAACTTTAAGAAGGAGATATACATATGAATTCTAAGAGTGCCCAGGGTC) and OVL188R (AGTGCGGCCGCTTAATGGTGATGGTGATGGTGCTCGAGTGCAGCTGCCATTCGGGAGGGCGGGCTGG) bearing SpeI and NotI restriction sites, respectively (underlined). The 1.1 kb PCR product was digested with SpeI and NotI and subcloned into XbaI/NotI sites of pET21a(+) *Escherichia coli* expression vector (Novagen, Madison, WI), immediately upstream of the His6 tag. The resulting plasmid, pUSP2-HIS, thus encoded USP2 fused to His6 tag at its C-terminus via an AAALE linker.[24] The construct pUSP2-HIS served as template to introduce mutations using the QuikChange XL Site-Directed Mutagenesis Kit (Stratagene, La Jolla, CA) according to the manufacturer's protocol. The mutagenic primers are listed in Supporting Information Table 1. All introduced mutations were confirmed by DNA sequencing.

**Expression and Purification of Wild-Type and Mutant USP2 Proteins.** Wild-type and mutant USP2 were expressed in BL21(DE3) *E. coli* (Novagen) in LB containing 100 $\mu$g/mL ampicillin. One liter of LB broth (Schlicke and Brakmann., 2005) inoculated with 5 mL of overnight culture was grown at 37 °C until an $OD_{600}$ value of 0.6−0.8 was reached. Expression of the recombinant protein was induced with 0.3 mM IPTG (isopropyl-1-thio-$\beta$-D-galactopyranoside) at 30 °C for 3 h.

Recombinant proteins were purified using a His-Bind Purification Kit (Novagen) according to the instructions of the supplier. Briefly, cell pellets were resuspended in 30 mL of lysis buffer (20 mM Tris-HCl, pH 8.0; 0.5 M NaCl, 0.1% triton X-100, 50 $\mu$M PMSF (Sigma)) and ruptured by sonication. The His-tagged proteins were purified in batch by incubating cell lysate with 1.5−2 mL of Ni−NTA resin for 1 h at 4 °C on a rotator, followed by several washes and elution using gravity columns. The eluted proteins were transferred into 20 mM Tris-HCl (pH 8.0), 10% (v/v) glycerol, and 1 mM DTT using a NAP-5 column (GE Healthcare, UK), aliquoted, and stored at −80 °C.

**Production of Ub-Based Substrates.** Construction of pTYB1-Ubiquitin$^{1-75}$ plasmid, which expresses Ubiquitin$^{1-75}$-Intein-CBD, has been described previously.[25] Ubiquitin-V$^{77}$-Intein-CBD was obtained by site-directed mutagenesis of pTYB1-Ubiquitin$^{1-75}$ using the QuikChange XL Site-Directed Mutagenesis Kit, and the sequence was confirmed by DNA sequencing. Expression of Ub-V$^{77}$-intein-CBD in BL21(DE3) *E. coli* (Novagen) was induced with 0.3 mM IPTG for 4 h at 30 °C. Cell pellets from 2 L of culture were resuspended in 45 mL of lysis buffer (20 mM Tris-HCl, pH 8.0, 0.5 M NaCl, 0.1% Triton X-100, and 50 $\mu$M PMSF) and were lysed by sonication. Following centrifugation at 30000*g* for 30 min, the clarified lysate was mixed with 4 mL of Chitin-Sepharose beads (New England Laboratories), equilibrated with lysis buffer for 30 min at 4 °C with agitation. After binding of the fusion protein, the lysate−beads mixture was loaded onto a 1.6 × 10 cm column and the flow-through collected. The beads were washed thoroughly with lysis buffer to remove unbound proteins and then equilibrated with a column buffer (20 mM Tris-HCl, pH 8.5, 500 mM NaCl). Column buffer containing 50 mM DTT was then added to the column, and the fusion protein incubated overnight (∼16 h) at 4 °C for on-column cleavage to occur. Ub-V$^{77}$ was eluted with column buffer, and the collected fraction was concentrated to 2 mL using a Biomax-5 membrane (Millipore). Protein concentration of Ub-V$^{77}$ was determined by Pierce Microplate BCA Protein Assay Kit (Thermo Pierce Biotechnology). Production of Ub-AMC was carried out as previously described.[25] The identities (MW) of the purified Ub-V$^{77}$ and Ub-AMC products were confirmed by mass spectrometry.

**In Vitro Deubiquitination Assays.** For enzyme kinetics measurements, the protein concentration of each USP2 protein was determined by Bradford, the surface area in a LC-MS elution profile, and active site titration by the inhibitor Ub-Vinyl Methyl Ester (Ub-VME). The latter method was the preferred one, and comparison with LC-MS traces was used to confirm the relative concentrations of all mutants. The activity of purified USP2 wild-type and mutants was first assessed using the fluorogenic substrate Ub-AMC. The rate of substrate hydrolysis was determined by monitoring the increase in AMC-released fluorescence emission at 440 nm ($\lambda_{ex}$ = 380 nm) as a function of time on a SPEX Fluorolog-2 spectrofluorometer (Horiba Jobin Yvon, Edison, NY). The kinetic measurements were carried out in 50 mM Tris-HCl (pH 7.8) containing 2 mM dithiothreitol (DTT), 200 mM NaCl, and 2% (v/v) dimethyl sulfoxide, at 25 °C. Reactions were initiated by the addition of the enzyme. Initial rates of substrate hydrolysis were determined at various substrate concentrations, and the data were fitted to the Michaelis−Menten equation to determine the kinetic parameters $k_{cat}$ and $K_M$. Substrate hydrolysis was also evaluated by monitoring full progress curves (i.e., by allowing complete hydrolysis of the substrate) at $[S] \ll K_M$, as described previously.[25]

**Peptidase and Isopeptidase Activity Determination by LC-MS.** The hydrolysis of label-free ubiquitin substrates Ub-(K$^{48}$C)-Ub-D$^{77}$ (Enzo Life Sciences Int.) and Ub-V$^{77}$ was monitored by mass spectrometry. The reactions were carried out at 6 $\mu$M of substrate in 50 mM Tris-HCl (pH 7.8), 200 mM NaCl, 2 mM DTT, and 0.1 mg/mL ovalbumin at room temperature. After the addition of the enzyme (typically 50 nM), aliquots were taken at various time intervals and mixed with 10 $\mu$L of stop solution (80:20:1, water:acetonitrile:formic acid). The disappearance of substrate and concomitant appearance of product were monitored by LC-MS on an Agilent 1200 HPLC system coupled to an Agilent QQQ6410 mass spectrometer. The system was controlled by MassHunter workstation software. Separation was performed on a POROSHELL 300SB-C18 column (5 $\mu$m, 2.1 × 75 mm, Agilent Technologies). The gradient used to separate the substrate Ub(K$^{48}$C)-Ub-D$^{77}$ and its corresponding hydrolysis products consisted of solvent A (97:3:0.2, water:acetonitrile:formic acid) and solvent B (87:10:3:0.2, acetonitrile:methanol:water:formic acid), starting at 10% B for 0.6 min, ramping to 75% B over 7.4 min and holding at 75% B

for 0.8 min, back to initial condition in 0.1 min, and then equilibrating for 1 min. The gradient used for substrate Ub-$V^{77}$, and its products consisted of solvent A (97:3:0.2, water:acetonitrile:formic acid) and solvent B (77:20:3:0.2, acetonitrile:methanol:water:formic acid) starting at 20% B for 0.6 min, ramping to 35% B over 9.4 min, ramping to 75% B over 0.1 min, and holding for 1 min, back to 20% B in 0.1 min, and then equilibrating for 1 min. The initial flow rate was set at 0.8 mL/min (or 1 mL/min for Ub($K^{48}C$)-Ub-$D^{77}$) and was increased after 8−10 min to 2 mL/min. The column was maintained at 70 °C, and the injection volume was 1 $\mu$L. Ionization was achieved using electrospray in positive mode with the spray voltage set at 4500 V. Nebulizer pressure ($N_2$) was set at 55 psi with a source temperature of 100 °C. Desolvation gas ($N_2$) was heated to 350 °C and delivered at 12 L/min. The fragmentor energy was 135 V. Full MS2 scan from 500 to 1300 $m/z$ was performed, and data were processed using Qualitative analysis software.

**Multiple Sequence Alignment.** Sequences of the currently known human USPs corresponding to the C19 family of the MEROPS peptidase database were collected from the GenBank and SwissProt databases. Only one sequence was selected from those of multiple isoforms reported for some USPs, thus leading to a nonredundant set of 54 distinct human USP sequences. The boundaries of their catalytic core were obtained from the Pfam and InterPro databases and confirmed, whenever available, with actual structures retrieved from the Protein Data Bank (PDB) with PDB IDs for USP2 (2HD5, 2IBI), USP7 (1NB8, 1NBF, 2F1Z), USP8 (2GFO), and USP14 (2AYN, 2AYO). The 54 catalytic core sequences were subjected to a multiple sequence alignment performed with the MAFFT 5 program[26] with the L-INS-i iterative refinement algorithm and visualized using Jalview 2.4.0B2.[27]

**Molecular Dynamics Simulations.** We carried out molecular dynamics (MD) simulations in explicit solvent for the catalytic core of USP2, free as well as complexed with Ub-$\varepsilon$Lys, as tetrahedral intermediate adduct. The 2.2 Å resolution crystal structure of complexed USP2 (PDB code 2IBI) was used as starting point for the simulations. Protonation state at physiological pH was adopted, except for the catalytic Cys considered ionized in the thiolate form in the uncomplexed USP2, and the catalytic His was considered protonated in both free and bound USP2. Also, the four Cys residues coordinating the $Zn^{2+}$ ion in the nested Zn-finger domain were treated in the ionized form. Crystallographic water molecules buried or presumably catalytically important were retained (10 for free USP2, 28 for complexed USP2).

For the USP2-Ub-$\varepsilon$Lys adduct, a cysteine tetrahedral intermediate (CTI) amino acid residue (see Supporting Information Figure 1) was constructed and parametrized. The CTI residue was constructed starting from the thiohemicetal adduct of the USP2 active site Cys residue bound to the Gly75-glycinealdehyde terminal segment of Ubal in the 2IBI crystal structure. A Lys residue was built off the tetrahedral C center of the thiohemiacetal adduct starting with the side-chain $\varepsilon$-amino N atom, thus effectively mimicking the cleavage of an isopeptide scissile bond. After the entire N$\varepsilon$-linked Lys was built from standard geometries in Sybyl 8 (Tripos, Inc., St. Louis, MO) in an extended conformation not colliding with USP2 atoms, the CTI fragment was extracted from the USP2-Ubal context and blocked at its five attachment positions with acetyl and aminomethyl groups (Supporting Information Figure 1). Blocked CTI residue was subjected to partial charge calculations by the two-stage restrained fitting procedure, RESP,[28] to the electrostatic potential calculated at the 6-31G* *ab initio* level using GAMESS.[29] Final partial charges for the unblocked CTI to be used in MD simulations were obtained by normalization of RESP charges to $-1e$ net charge.

Classical MD simulations were carried out under the AMBER force field with the FF99SB parameters[30,31] using the AMBER 10 software.[32,33] Appropriate force field atom types for the CTI residue were assigned with the ANTECHAMBER program in AMBER 10. Each prepared structure was solvated in a truncated octahedron TIP3P water box,[34] and electroneutrality was achieved by adding $Cl^-$ counterions. Applying harmonic restraints with force constants of 10 kcal/(mol Å$^2$) to all solute atoms, the system was energy-minimized first, followed by heating from 100 to 300 K over 25 ps in the canonical ensemble (constant number of particles, volume, and temperature, NVT) and by equilibrating to adjust the solvent density under 1 atm pressure over 25 ps in the isothermal−isobaric ensemble (constant number of particles, pressure, and temperature, NPT) simulation. The harmonic restraints were then gradually reduced to 0 with four rounds of 25 ps simulations. A 10 ns production NPT run was obtained with snapshots collected every 1 ps, using a 2 fs time step and 9 Å nonbonded cutoff. The particle mesh Ewald method[35] was used to treat long-range electrostatic interactions, and bond lengths involving bonds to hydrogen atoms were constrained by SHAKE.[36] The $Zn^{2+}$ ion in the Zn-finger domain was restrained within the 2.2−2.7 Å range from each of its four coordinating cysteine S atoms using a harmonic potential with a force constant of 30 kcal/(mol Å$^2$) during the course of simulation. Standard analyses of MD trajectories were carried out with PTRAJ in AMBER 10. The MD simulations of both free and complexed USP2 attained structural convergence (Supporting Information Figure 2).

## RESULTS AND DISCUSSION

**Production of USP2 Active Site Mutants.** To gain a detailed understanding of the specific roles played by residues found at the active site, we used site-directed mutagenesis to generate a number of USP2 variants. The residues found at the active site and targeted for mutation are illustrated in Figure 2. In a first round of mutagenesis, residue Asn271, believed to form part of the oxyanion hole of USP2, and its interacting partner Asp575, were mutated to Ala to generate the USP2 variants Asn271Ala and Asp575Ala as well as a double mutant Asn271Ala/Asp575Ala. Both residues are absolutely conserved in all but one USP sequence (Figure 1). A second round of mutagenesis focused on residues reported to constitute the catalytic triad of USP2, i.e., Cys276, His557, and Asn574 (Figure 2). Asn574, the "third member" of the triad, is not fully conserved, being present in ∼50% of USP sequences (Figure 1). Its neighboring residue, however, Asp575, is well conserved in all USPs. Given these observations, we generated single alanine mutants of each of the residues of the catalytic triad as well as a double mutant Asn 574Ala/Asp575Ala.

All the USP2 mutants were expressed in *E. coli* as His-tag fusion proteins and were subsequently affinity-purified on a Ni-NTA column followed by gel filtration chromatography on NAP-5 to yield a single band on SDS-PAGE (Supporting Information Figure 3). All purified USP2 variants were analyzed by LC-MS and displayed a single peak in their elution profiles. The molecular masses of the USP2-HIS variants obtained from the ESI mass spectra were all in agreement with the predicted MW (Supporting Information Figure 4).

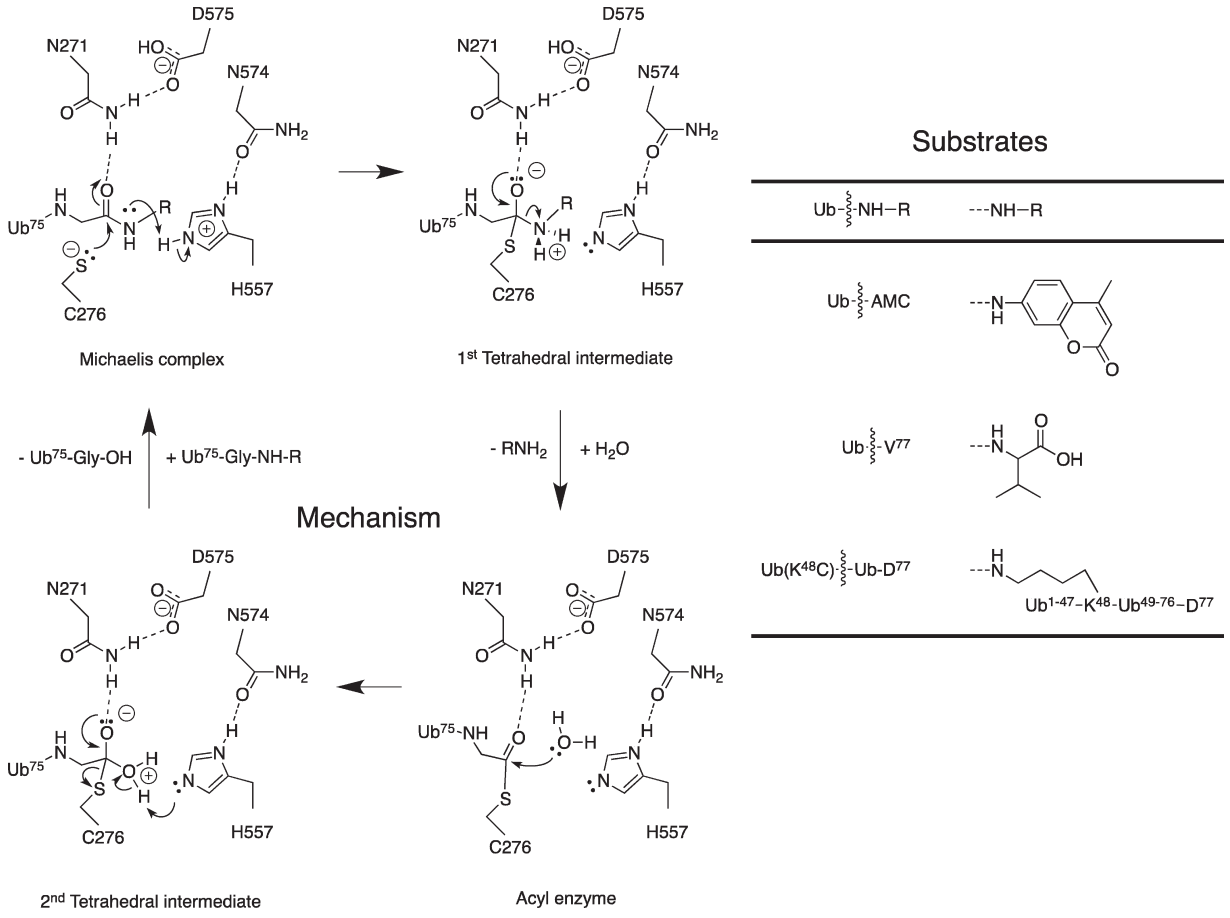


**Figure 2.** Catalytic mechanism. The C-terminal Gly of ubiquitin is explicitly shown. The leaving group after the first tetrahedral intermediate is a neutral RNH2. This makes AMC a better leaving group over Lys isopeptide and Val. The latter are not in their preferred protonated state of having positively charged aliphatic amines whereas the aromatic amine in AMC is already in its preferred state. From the acyl enzyme onward the steps are identical regardless of substrate. Detailed structures of the leaving groups are shown on the right for the various substrates.

**Table 1. Kinetic Parameters for Hydrolysis of Ub-AMC by USP2 Variants**

| enzyme | $k_{cat}$ ($s^{-1}$) | $K_M$ ($\mu$M) | $k_{cat}/K_M$ ($10^5$ $M^{-1}$ $s^{-1}$) |
|---|---|---|---|
| wild-type | 0.623 ± 0.079 | 2.49 ± 0.28 | 2.50 ± 0.42 |
| **oxyanion hole mutants** | | | |
| Asn271Ala | 0.77 ± 0.11 | 2.15 ± 0.28 | 3.56 ± 0.68 |
| Asp575Ala | 0.054 ± 0.006 | 0.276 ± 0.028 | 1.96 ± 0.31 |
| Asn271Ala/Asp575Ala | 0.234 ± 0.036 | 1.88 ± 0.22 | 1.24 ± 0.24 |
| **catalytic triad mutants** | | | |
| Cys276Ala | inactive | | |
| His557Ala | inactive | | |
| Asn574Ala | 2.00 ± 0.35 | 4.88 ± 0.85 | 4.1 ± 1.0 |
| Asn574Ala/Asp575Ala | 0.099 ± 0.009 | 0.992 ± 0.087 | 1.00 ± 0.13 |

**Contribution of Putative Oxyanion Hole Residues to Substrate Hydrolysis by USP2.** To characterize the enzymatic activity of USP2 and its variants, we first used a general assay for deubiquitinating enzymes based on the substrate Ub-AMC. The kinetic parameters obtained for the wild-type and mutant enzymes are reported in Table 1. Wild-type USP2 hydrolyzes Ub-AMC with a $k_{cat}/K_M$ of $2.50 \times 10^5$ $M^{-1}$ $s^{-1}$, in agreement with previously published value.[24] Very little effect on activity is seen for either of the single mutants Asn271 and Asp575, or even for the Asn271/Asp575 double mutant, indicating that these residues do not affect the overall catalytic efficiency toward Ub-AMC. For one mutant, Asp575Ala, a 10-fold decrease in $k_{cat}$ is observed. However, this is mostly compensated for by a decrease in $K_M$ (Table 1). Contrary to our finding, a previous study found that mutation of Asn218 in the oxyanion hole of USP7 significantly decreased activity against a Lys48-linked diubiquitin substrate.[21] To examine if the role of these residues could be dependent on the nature of the substrate, we used mass spectrometry


dx.doi.org/10.1021/bi101958h |*Biochemistry* 2011, 50, 4775–4785

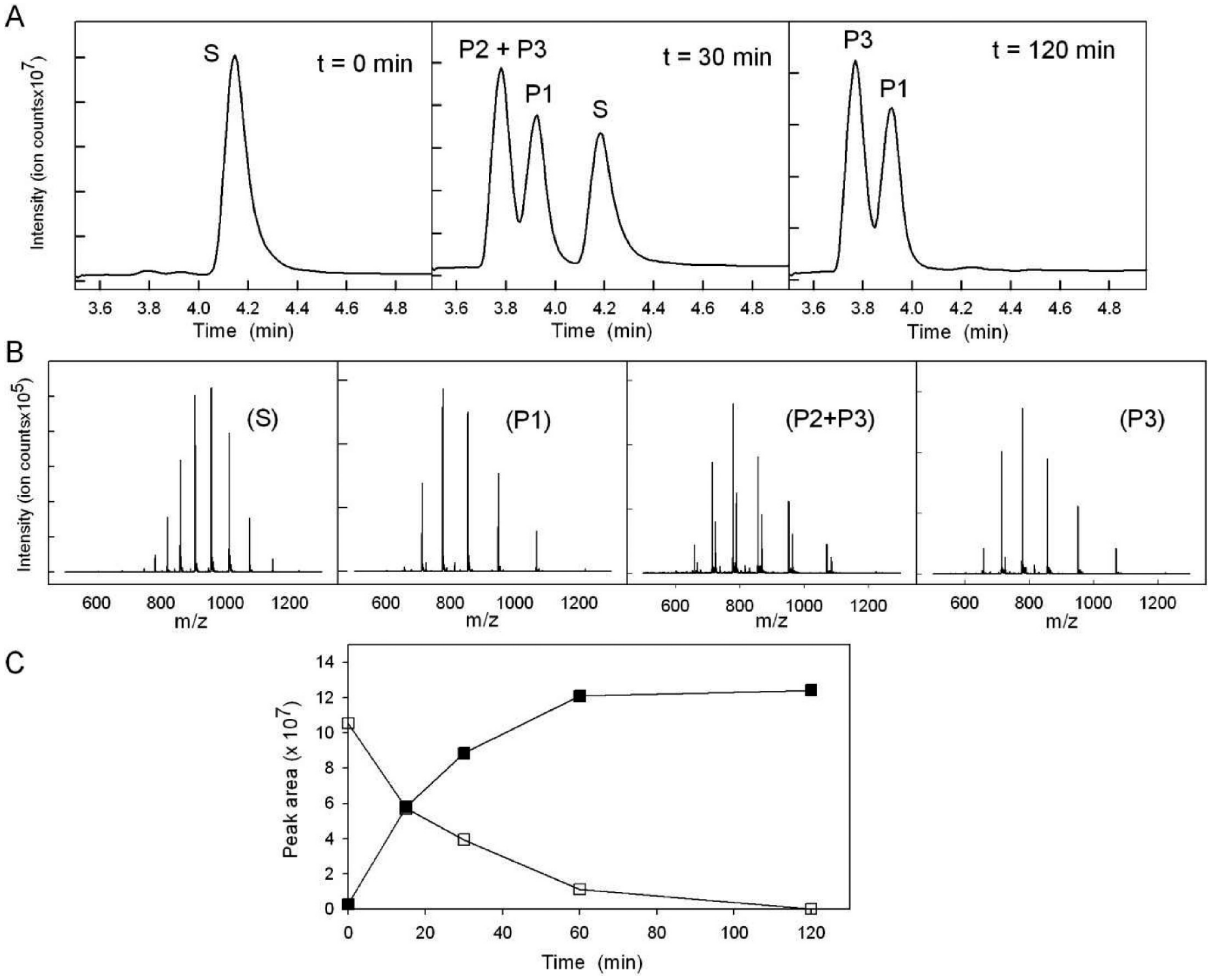


**Figure 3.** LC-MS based assay for determination of isopeptidase activity. (A) LC trace for hydrolysis of Ub($K^{48}C$)-Ub-$D^{77}$ by wild-type USP2 for incubation times of 0, 30, and 120 min. Conditions were as described in Materials and Methods. Two peaks were observed to account for the three possible products of the reaction. (B) MS spectra corresponding to each peak observed in the LC trace. S: substrate (MW = 17 202.3 Da vs 17 201.7 Da theoretical); P1: Ub($K^{48}C$) (MW = 8539.7 Da vs 8539.8 Da theoretical); P2: Ub-$D^{77}$ ((MW = 8680.0 Da vs 8679.9 Da theoretical); P3: Ub (MW = 8564.6 Da vs 8564.8 Da theoretical). At intermediate times (e.g., 30 min), the first peak of the LC trace contains two products: P2 and P3, while at $t$ = 120 min, the peak corresponds to P3 only. (C) Time course for disappearance of substrate (□) and appearance of product Ub($K^{48}C$) (■). The relative amount of each compound is taken from the surface area of the corresponding peak in the LC trace.

to monitor the cleavage of the isopeptide bond in a synthetic diubiquitin substrate. Initial tests using commercial diubiquitin were not conclusive due to the presence of a nonhydrolyzable contaminant. This contaminant was identified by X-ray crystallography as a cyclized diubiquitin variant, where the C-terminal glycine of the proximal Ub is conjugated to the Lys48 side-chain of the distal Ub (data not shown). To overcome this problem, we made use of a noncyclizable derivative, Ub($K^{48}C$)-Ub-$D^{77}$ to implement the label-free MS assay. USP2 was incubated with Ub($K^{48}C$)-Ub-$D^{77}$, and the conversion of the substrate to products was analyzed by LC-MS. Hydrolysis of this substrate by USP2 can generate three different Ub variant products: Ub($K^{48}C$), Ub-$D^{77}$, and Ub. As shown in Figure 3, the peaks corresponding to the substrate and products can be resolved by LC (with the exception of Ub and Ub-$D^{77}$), and their identity was confirmed by MS. Peak (P2 + P3) observed in the earlier stages of the reaction (e.g., at 30 min, Figure 3A) contains both Ub-$D^{77}$ and Ub, indicating that cleavage of the Ub-Ub isopeptide bond is faster than cleavage of the peptidyl Ub-$D^{77}$ bond. After longer incubation times, only Ub($K^{48}C$) and Ub are observed. It was not possible to dissect out individual rate constants, but the disappearance of substrate or appearance of product Ub($K^{48}C$) can be used to monitor the activity of USP2 and its variants (Figure 3C).

The results obtained for the hydrolysis of Ub($K^{48}C$)-Ub-$D^{77}$ by the oxyanion hole mutants Asn271Ala, Asp575Ala, and Asn271Ala/Asp575Ala are presented in Figure 4A. Mutation of Asp575 to Ala has no effect on enzyme activity. However, contrary to the results obtained with Ub-AMC, a significant decrease in activity is observed for both Asn271Ala and Asn271Ala/Asp575Ala variants, with the double mutant being the least active. To verify if the nature of the bond cleaved (peptide vs isopeptide) could be responsible for the difference, we have used the same MS-based assay to monitor hydrolysis of a substrate which does not contain an isopeptide bond, Ub-$V^{77}$ (Figure 4B). The results obtained for the two substrates, compared in Figure 4C, indicate that the same trend is observed with the Ub-$V^{77}$ substrate; i.e., Asp575Ala remains fully active while the most important decrease in activity is obtained with the double mutant. These results implicate a role for the Asn271-Asp575 pair in formation of an oxyanion hole to stabilize the transition state in substrate hydrolysis.


dx.doi.org/10.1021/bi101958h |*Biochemistry* 2011, 50, 4775–4785

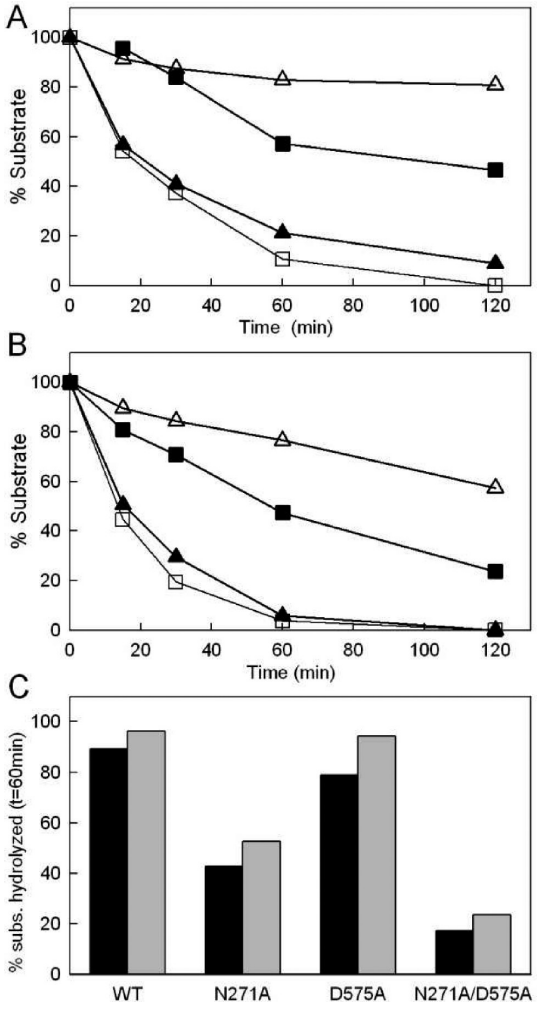


**Figure 4.** Hydrolysis of Ub($K^{48}C$)-Ub-$D^{77}$ (A) and Ub-$V^{77}$ (B) by USP2 oxyanion hole mutants. Time courses for the reactions are expressed as percentage of substrate remaining as a function of time, for the wild-type (□), Asn271Ala (■), Asp575Ala (▲), and Asn271Ala/Asp575Ala (△) mutants. Reactions were carried out as described in Materials and Methods. (C) Percentage of substrate hydrolysis observed at $t$ = 60 min incubation for the Ub($K^{48}C$)-Ub-$D^{77}$ (black bars) and Ub-$V^{77}$ (gray bars) substrates.

This difference between Ub-AMC and ubiquitin peptide/isopeptide substrates, particularly the insensitivity of Ub-AMC to USP2 oxyanion hole mutants, is interesting and intriguing. Mechanistically, the difference must be related to the acylation step of hydrolysis, since the deacylation step is identical between all these substrates (Figure 2). Moreover, while both acylation and deacylation steps proceed via a tetrahedral intermediate (TI) involving an oxyanion (first and second tetrahedral intermediates in Figure 2), the stability of the deacylation TI depends less on the oxyanion hole residues since, due to steric considerations, the second TI can exist in the alternate configuration in which the oxyanion can be stabilized by the protonated catalytic His. This mirrors to some extent the conformational duality of aldehyde inhibitor adducts with related papain-like cysteine proteases.[37] It is the TI of the acylation step in which the oxyanion must be accommodated in the oxyanion hole due to steric constraints (the bulky NH-R leaving group of the substrate does not fit into the oxyanion hole). Hence, oxyanion hole mutations can affect the overall catalysis, but their effect will likely be reduced if acylation is not the rate-limiting step. The hydrolysis of a dipeptidyl-AMC substrate by cathepsin C, an aminodipeptidase of the papain family, has been shown to involve an acylation step that is about 10-fold faster than the rate-limiting deacylation.[38] In this case, for example, the effects of oxyanion hole mutants that impair the stabilization of acylation TI by 10-fold or less would not be detected. Such a scenario is consistent with our Ub-AMC hydrolysis data by USP2. For papain, mutation of the oxyanion hole Gln19 to alanine, for example, affected hydrolysis of an AMC substrate by 60-fold (mainly $k_{cat}$),[39] but the net impact on the acylation step would be even larger if the deacylation step is indeed rate-limiting. In the case of the USP2-catalyzed hydrolysis, we see here a decreased sensitivity of hydrolysis to oxyanion hole mutations for the AMC substrate relative to the other peptide/isopeptide substrates used. This implies a rebalance of the acylation/deacylation rates for different substrates. This is expected from a chemical point of view, since the aliphatic leaving group (amine) of the peptide/isopeptide substrates depends more on protonation (by the catalytic His) than the aromatic amine departing from the AMC substrate. Hence, slower acylation for hydrolysis of Ub-($K^{48}C$)-Ub-$D^{77}$ and Ub-$V^{77}$ could explain why increased sensitivity to oxyanion hole stabilization is observed for these substrates compared to hydrolysis of the Ub-AMC.

**Structural Roles of Conserved Putative Oxyanion Hole Residues.** Crystal structures of the catalytic cores of several USPs have been solved in the unbound state, in complex with ubiquitin, or bound to inhibitors (e.g., ubiquitin aldehyde, Ubal). While such complexes can potentially instruct on enzyme−substrate interactions and specific roles in catalysis, they also have certain limitations. In the case of USP2−ubiquitin complex (PDB code 2HD5), due to the negative formal charge at the C-terminal Gly76 residue of ubiquitin, an apparent electrostatic repulsion with the active site thiolate resulted in an uncharacteristic conformation of the latter.[24] Structures of USPs solved as complexes with various ubiquitin-based inhibitors, primarily Ubal, were thought to shed light into the interactions of the resulting covalent thiohemiacetal adduct with putative oxyanion hole residues. As shown in Figure 5A for a model structure of USP2-Ubal adduct (based on the crystal structure of USP2 complexed as an irreversible adduct with ubiquitin(1−75)−ethylamine, PDB code 2IBI), a water molecule appears to bridge both the putative oxyanion hole residue Asn271 and the conserved Asp575 to the oxygen atom (modeled in the oxyanion hole) of the ensued thiohemiacetal; hence, only indirect specific interactions of the substrate with these residues are proposed. An important observation regarding this arrangement is that if the O atom of the thiohemiacetal would be in the ionized state (oxyanion), the bridging water molecule would be surrounded by three hydrogen-bonding acceptors (Figure 5A). This suggests that in an USP-Ubal adduct the thiohemiacetal would most likely be in the neutral protonation state (hydroxyl) acting as H-bond donor to the bridging water molecule. The situation is fully supported by the similar case of the USP7-Ubal complex (PDB code 1NBF) (see Supporting Information Figure 5). Hence, USP complexes inhibited by ubiquitin-based inhibitors like Ubal or other electrophilic ubiquitin-based probes, while relatively easy to trap and crystallize, may provide a limited and distorted view for the enzyme interactions with the oxyanion developing on the TI in the acylation step for the hydrolysis of a bona fide substrate.[39,40]

In order to better delineate oxyanion interactions in the acylation step, we modeled USP2 in complex with the isopeptide

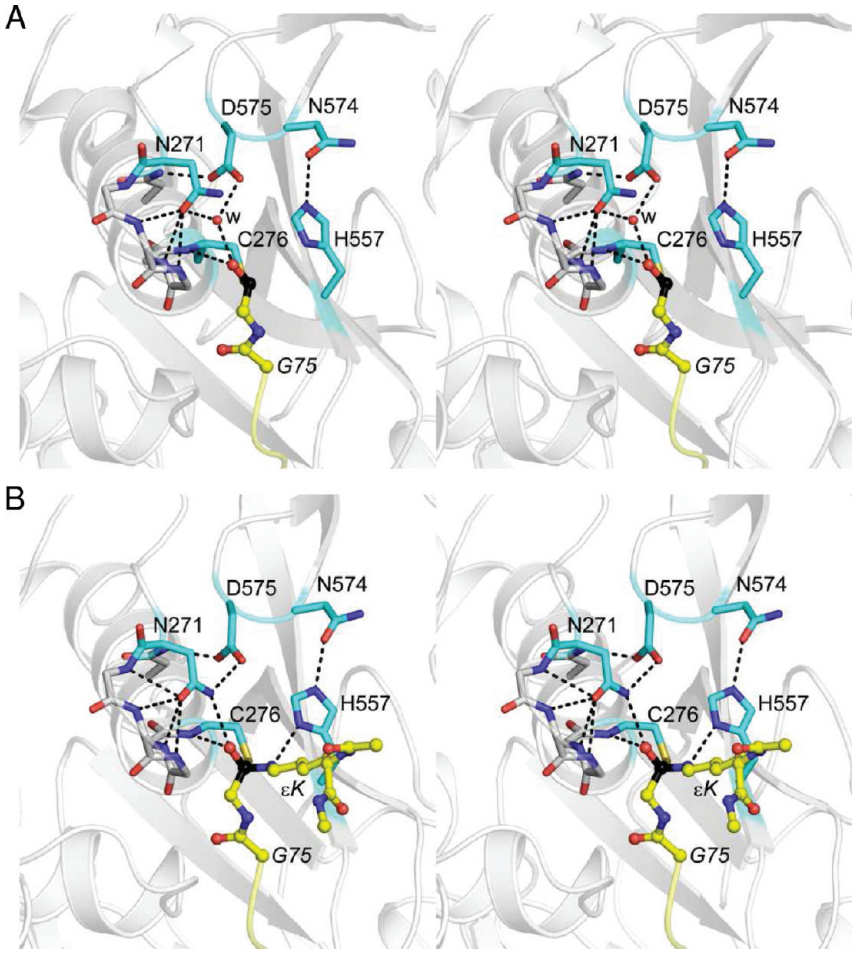


**Figure 5.** Oxyanion hole interactions. (A) X-ray structure of USP2 complexed as a covalent adduct with ubiquitin(1−75)-ethylamine (PDB code 2IBI). The thiohemicetal O atom that would be formed in a USP2-Ubal complex was modeled and projects into the oxyanion hole. (b) MD average minimized structure of USP2 in complex with Ub-εLys tetrahedral intermediate adduct. The average is taken over the 10th ns of the MD production run. USP catalytic core is shown as gray ribbon; Ubal and Ub-εLys are shown as yellow ribbons. Select USP2 side chains are shown as sticks, with the Gly75-glycinealdehyde fragment of Ubal adduct, and the Gly75-Gly76-εLys fragment of Ub-εLys adduct as ball-and-stick. Hydrogen bonds are indicated by dashed lines.

substrate Ub-εLys by MD simulations in explicit water. The complex was modeled as a TI at the active site Cys276 residue, with the ionized O atom of the thiohemiacetal projecting in the oxyanion hole. The active site geometry obtained from 10 ns of MD simulation is shown in Figure 5B. Although the USP2 crystal structure geometry (PDB code 2IBI) with the water molecule bridging to a modeled oxyanion was used as starting point, after less than 1 ns of MD simulation the bridging water was expelled and replaced by the side-chain $NH_2$ group of the conserved Asn271 residue, whose protons then established and maintained direct interactions with the oxyanion. This was effectively accomplished by a rotation of about 90° around the $\chi 2$ torsion angle in the Asn271 side chain. The Asn271 side-chain O atom maintained and even improved its H-bond interactions with several main-chain amide protons from the intervening loop up to the catalytic Cys276. Furthermore, the direct Asn27−oxyanion interaction is stabilized by an H-bond with the exposed O atom of the conserved Asp575 carboxylate group (while its buried O atom remains engaged in H-bonds with Asn279 and a buried water molecule). Nature has selected and conserved significantly the Asn271 and Asp575 residues to the same extent as the catalytic residues Cys276 and His557. From a structural viewpoint, conservation for these putative oxyanion hole residues appears justified. Notably, the oxyanion stabilization is accomplished in a similar fashion by the conserved oxyanion hole Gln residue in papain-like cysteine proteases and by the conserved Asn/Asp tandem in USPs. Specifically, the side-chain amide N and O atoms of Gln in papain-like enzymes overlap remarkably with the side-chain amide N atom of Asn and side-chain carboxylate O atom of Asp, respectively, of USPs (Supporting Information Figure 6B). This may indicate that the effect upon mutation of the conserved oxyanion hole Gln residue in papain-like enzymes (seen with AMC substrates)[39,41] would be matched by simultaneous mutation of the conserved Asn/Asp pair for oxyanion stabilization in USPs, providing a plausible explanation for the results observed with the Ub($K^{48}C$)-Ub-$D^{77}$ and Ub-$V^{77}$ substrates on USP2 oxyanion hole mutants.

This structural arrangement of Asn271, where it is poised for direct interaction with the oxyanion, and structurally supported by Asp575, is not novel, and has been observed in the crystal structures of unbound USPs that exhibit aligned catalytic triads, e.g., USP8 and USP14, which differ from USP structures with misaligned catalytic triad in the Ub-unbound state (e.g., USP7). Starting from the Ubal-complexed USP2 geometry, we also run 10 ns of MD simulation for free USP2 and obtained a catalytically

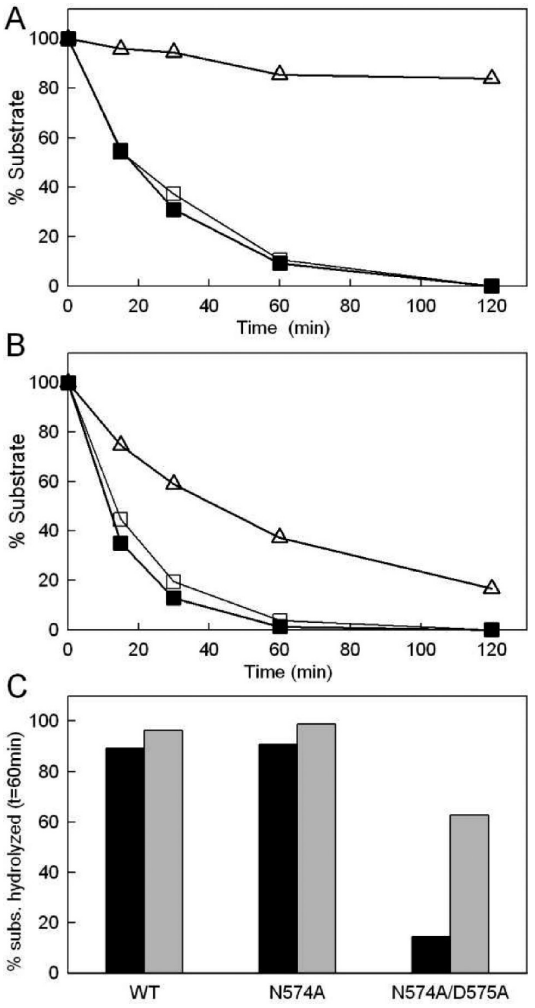


**Figure 6.** Hydrolysis of Ub($K^{48}$C)-Ub-$D^{77}$ (A) and Ub-$V^{77}$ (B) by USP2 catalytic triad mutants. Time courses for the reactions are expressed as percentage of substrate remaining as a function of time, for the wild-type (□), Asn574Ala (■), and Asn574Ala/Asp575Ala (△) mutants. Reactions were carried out as described in Materials and Methods. (C) Percentage of substrate hydrolysis observed at $t$ = 60 min incubation for the Ub($K^{48}$C)-Ub-$D^{77}$ (black bars) and Ub-$V^{77}$ (gray bars) substrates.

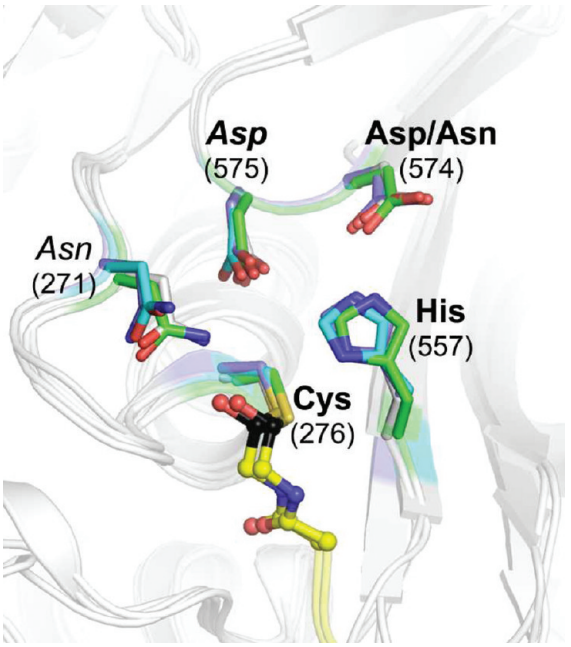


**Figure 7.** Overlay of human USP crystal structures with highlighted catalytic triad residues Cys, His, and Asp/Asn (bold labeling), conserved putative oxyanion hole residue Asn (italic labeling) and conserved Asp residue with putative dual supporting role (bold-italics labeling), and USP2 residue numbering given in parentheses. The thiohemicetal O atom that would be formed in a USP2-Ubal complex was modeled based on the X-ray structure of USP2 complexed as a covalent adduct with ubiquitin(1−75)-ethylamine (PDB code 2IBI). Bonds to C atoms are colored as following: USP2 (PDB code 2IBI) cyan, USP7 (1NBF) purple, USP8 (2GFO) green, USP14 (2AYN) gray. All USP catalytic cores are shown as gray ribbon, Ubal bound to USP2 and USP7 as yellow rendering with Gly75-glycinealdehyde fragment as ball-and-stick. USP2 has CHN triad, and USP7, USP8, and USP14 have CHD triads.

competent active site showing the same Asn271 flipping into a conformation poised for interaction with the oxyanion as in the USP−substrate complex, and as in the crystal structures of free USPs with aligned catalytic triads (see Supporting Information Figure 7). These observations indicate that free USP core domains can be poised to interact with the oxyanion directly via the side chain of the conserved Asn271 and that crystal structures of Ubal-bound USPs may be distorted due to the protonated form of the oxyanion,[39,40] which introduces an electrostatic repulsion with the Asn271 side-chain amide.

**Contribution of Catalytic Triad Residues to Substrate Hydrolysis by USP2.** Mutants of the catalytic triad residues (Cys276, His557, and Asn574) were characterized against the substrates Ub-AMC, Ub($K^{48}$C)-Ub-$D^{77}$, and Ub-$V^{77}$. As expected, mutation of Cys276 to Ala and His557 to Ala abolished activity against all three substrates used (Table 1). Interestingly, however, activity could be recovered for the His557Ala mutant when the medium contained imidazole at concentrations in the low millimolar range (data not shown). For the third member of the triad, however, the single mutation of Asn574 to Ala had no effect on activity for all three substrates tested (see Table 1 and Figure 6). With respect to the double mutant Asn574Ala/Asp575Ala, the results are once again dependent on the substrate used. Only very low residual activity could be detected for the diubiquitin substrate Ub($K^{48}$C)-Ub-$D^{77}$, and a significant decrease was also found with Ub-$V^{77}$, although of lower magnitude than that obtained with Ub($K^{48}$C)-Ub-$D^{77}$. However, with the Ub-AMC substrate, only a 2-fold decrease in $k_{cat}/K_M$ was observed. Interestingly, similar to the situation with the Asp575Ala mutant, the value of $k_{cat}$ and $K_M$ both decrease by a factor of 6 and 2.5, respectively, for the Asn574Ala/Asp575Ala double mutant.

Our results with USP2 on the single alanine mutation of the third member of the triad, Asn574, is in contrast with the previous data on the alanine mutation of the corresponding triad member Asp481 of USP7 that lead to undetectable activity based on an in vitro Lys-48 diubiquitin cleavage gel-based assay.[21] It is possible that the Asp481Ala mutant of USP7 is not as inactive as the qualitative gel-based assay may suggest, and significant residual activity may be detected with an MS-based assay. However, it must be recognized that the neighboring Asn574 and Asp575 residues in USP2 are replaced by two Asp residues in USP7, and this arrangement of residues might respond differently to mutations. Nevertheless, our data on USP2 indicate that


dx.doi.org/10.1021/bi101958h |*Biochemistry* 2011, 50, 4775–4785

its residue Asn574 does not represent the third member of a cysteine protease catalytic triad from a functional point of view.

There is structural data that seem to support this notion. For example, there are three types of triads in human USPs that are known or likely to be active: CHN, CHD, and CHS (Figure 1). The first type is characteristic to papain-like cysteine proteases. In human USPs, the CHN and CHD triads have ~50% occurrence each, and there appear to be no mutation(s) correlated with their occurrence. Particularly interesting is that activity has been confirmed for two USPs with Ser as the third member of the triad.[13] Crystal structures solved for several USPs in free or complexed state (CHN: USP2 and yeast Ubp6, CHD: USP7, USP8, and USP14) show no difference between the arrangement of the catalytic triad with respect to the third member being either Asn or Asp (Figure 7). The alanine mutation of the corresponding Asn175 in papain leads to an important reduction in catalytic efficiency, ~3000-fold, mostly affecting $k_{cat}$.[42] In papain-like enzymes, this Asn residue is buried and engaged in amide−aromatic interactions important for substrate binding and catalysis, besides a structural-orientation role implicated in the stability of the catalytic ion pair.[43] The S′ area in USPs is different from other papain-like homologues. In particular, contrary to cathepsins, the third member of the triad is exposed to the solvent, which argues for a diminished role of this residue relative to papain. In conclusion, structural analysis appears to suggest that the third member of the USP catalytic triad may not have a significant role in deubiquitination efficiency. Consistent with this notion is the variation in the third member of the triad for other DUBs, for example, Asp in yeast otubain-1,[44] Asn in otubain-2 (two residues, Asn226 and Thr45, stabilize the catalytic His224),[45] and a main-chain carbonyl group in A20.[46]

The decrease in activity for the USP2 double mutant Asn574Ala/Asp575Ala against the isopeptide substrate might indicate a reinforcing mechanism between these two residues in maintaining His557 in catalytically competent geometry and protonation state. Mutation of either Asn574 or Asp575 alone has no effect on USP2 activity (Figures 4 and 6). Both these side chains are in contact with the catalytic His557 imidazole ring (Figures 5 and 7). Hence, while removal of either side chain alone is not sufficient to ablate catalytic activity, deletion of both may destabilize the correct alignment and protonation of His557 for catalytic competency. This may include (i) ion-pair formation with the catalytic Cys226 and (ii) protonation of the leaving group amine. The Cys-His ion pair might exist in the free enzyme or might be formed after substrate binding in the Michaelis complex, as was suggested for UCH-L1.[47] Our data showing insensitivity of the AMC substrate to the USP2 double mutation Asn574Ala/Asp575Ala in contrast to the decrease in activity for the isopeptide substrate points to the second role, owing to different protonation requirements for the leaving groups of the two substrates leading to faster (and possibly non-rate-limiting) acylation with the AMC substrate. In conclusion, Asp575 emerges as an important conserved residue that may have a dual supporting role, in the formation of the oxyanion hole and in maintaining the correct alignment and protonation of His557 for catalytic competency.

## ■ ASSOCIATED CONTENT

**Supporting Information.** Details of protein purification and characterization, molecular dynamics simulations, and additional structural analysis. This material is available free of charge via the Internet at http://pubs.acs.org.

## ■ AUTHOR INFORMATION

### Corresponding Author

*Phone: (514) 496-6317. Fax: (514) 496-5143. E-mail: robert.menard@cnrc-nrc.gc.ca (R.M.); liyx486@nenu.edu.cn (Y.L.).

### Notes

[†]NRCC publication no. 53144.

### Funding Sources

This work was supported in part by a training fellowship from the Northeast Normal University and China Scholarship Council (to W.Z.).

## ■ ADDITIONAL NOTE

[a] In the text, USP2 refers to the catalytic domain of USP2, comprising residues Asn258 to Met605 (USP2 isoform 1 (USP2a) numbering).

## ■ REFERENCES

(1) Hershko, A., and Ciechanover, A. (1998) The ubiquitin system. *Annu. Rev. Biochem. 67*, 425–479.

(2) Hicke, L. (2001) Protein regulation by monoubiquitin. *Nat. Rev. Mol. Cell Biol. 2*, 195–201.

(3) Pickart, C. M., and Eddins, M. J. (2004) Ubiquitin: structures, functions, mechanisms. *Biochim. Biophys. Acta 1695*, 55–72.

(4) Pickart, C. M. (2001) Mechanisms underlying ubiquitination. *Annu. Rev. Biochem. 70*, 503–533.

(5) Weissman, A. M. (2001) Themes and variations on ubiquitylation. *Nat. Rev. Mol. Cell Biol. 2*, 169–178.

(6) Dye, B. T., and Schulman, B. A. (2007) Structural mechanisms underlying posttranslational modification by ubiquitin-like proteins. *Annu. Rev. Biophys. Biomol. Struct. 36*, 131–150.

(7) Glickman, M. H., and Ciechanover, A. (2002) The ubiquitin-proteasome proteolytic pathway: destruction for the sake of construction. *Physiol. Rev. 82*, 373–428.

(8) Pickart, C. M., and Fushman, D. (2004) Polyubiquitin chains: polymeric protein signals. *Curr. Opin. Chem. Biol. 8*, 610–616.

(9) Haglund, K., and Dikic, I. (2005) Ubiquitylation and cell signaling. *EMBO J. 24*, 3353–3359.

(10) Welchman, R. L., Gordon, C., and Mayer, R. J. (2005) Ubiquitin and ubiquitin-like proteins as multifunctional signals. *Nat. Rev. Mol. Cell Biol. 6*, 599–609.

(11) Wilkinson, K. D. (1997) Regulation of ubiquitin-dependent processes by deubiquitinating enzymes. *FASEB J. 11*, 1245–1256.

(12) Amerik, A. Y., and Hochstrasser, M. (2004) Mechanism and function of deubiquitinating enzymes. *Biochim. Biophys. Acta 1695*, 189–207.

(13) Nijman, S. M., Luna-Vargas, M. P., Velds, A., Brummelkamp, T. R., Dirac, A. M., Sixma, T. K., and Bernards, R. (2005) A genomic and functional inventory of deubiquitinating enzymes. *Cell 123*, 773–786.

(14) Reyes-Turcu, F. E., and Wilkinson, K. D. (2009) Polyubiquitin binding and disassembly by deubiquitinating enzymes. *Chem. Rev. 109*, 1495–1508.

(15) Rawlings, N. D., Morton, F. R., Kok, C. Y., Kong, J., and Barrett, A. J. (2008) MEROPS: the peptidase database. *Nucleic Acids Res. 36*, D320–D325.

(16) Ventii, K. H., and Wilkinson, K. D. (2008) Protein partners of deubiquitinating enzymes. *Biochem. J. 414*, 161–175.

(17) Wilkinson, K. D. (2009) DUBs at a glance. *J. Cell Sci. 122*, 2325–2329.

(18) Singhal, S., Taylor, M. C., and Baker, R. T. (2008) Deubiquitylating enzymes and disease. *BMC Biochem. 9* (Suppl 1), S3.

(19) Hussain, S., Zhang, Y., and Galardy, P. J. (2009) DUBs and cancer: the role of deubiquitinating enzymes as oncogenes, non-oncogenes and tumor suppressors. *Cell Cycle 8*, 1688–1697.

(20) Sacco, J. J., Coulson, J. M., Clague, M. J., and Urbé, S. (2010) Emerging roles of deubiquitinases in cancer-associated pathways. *IUBMB Life 62*, 140–157.

(21) Hu, M., Li, P., Li, M., Li, W., Yao, T., Wu, J. W., Gu, W., Cohen, R. E., and Shi, Y. (2002) Crystal structure of a UBP-family deubiquitinating enzyme in isolation and in complex with ubiquitin aldehyde. *Cell 111*, 1041–1054.

(22) Hu, M., Li, P., Song, L., Jeffrey, P. D., Chenova, T. A., Wilkinson, K. D., Cohen, R. E., and Shi, Y. (2005) Structure and mechanisms of the proteasome-associated deubiquitinating enzyme USP14. *EMBO J. 24*, 3747–3756.

(23) Avvakumov, G. V., Walker, J. R., Xue, S., Finerty, P. J., Jr., Mackenzie, F., Newman, E. M., and Dhe-Paganon, S. (2006) Amino-terminal dimerization, NRDP1-rhodanese interaction, and inhibited catalytic domain conformation of the ubiquitin-specific protease 8 (USP8). *J. Biol. Chem. 281*, 38061–38070.

(24) Renatus, M., Parrado, S. G., D'Arcy, A., Eidhoff, U., Gerhartz, B., Hassiepen, U., Pierrat, B., Riedl, R., Vinzenz, D., Worpenberg, S., and Kroemer, M. (2006) Structural basis of ubiquitin recognition by the deubiquitinating protease USP2. *Structure 14*, 1293–1302.

(25) Lindner, H. A., Lytvyn, V., Qi, H., Lachance, P., Ziomek, E., and Ménard, R. (2007) Selectivity in ISG15 and ubiquitin recognition by the SARS coronavirus papain-like protease. *Arch. Biochem. Biophys. 466*, 8–14.

(26) Katoh, K., Kuma, K., Toh, H., and Miyata, T. (2005) MAFFT version 5: improvement in accuracy of multiple sequence alignment. *Nucleic Acids Res. 33*, 511–518.

(27) Waterhouse, A. M., Procter, J. B., Martin, D. M., Clamp, M., and Barton, G. J. (2009) Jalview Version 2- a multiple sequence alignment editor and analysis workbench. *Bioinformatics 25*, 1189–1191.

(28) Bayly, C. I., Cieplak, P., Cornell, W. D., and Kollman, P. A. (1993) A well-behaved electrostatic potential based method using charge restraints for deriving atomic charges: The RESP model. *J. Phys. Chem. 97*, 10269–10280.

(29) Schmidt, M. W., Baldridge, K. K., Boatz, J. A., Elbert, S. T., Gordon, M. S., Jensen, J. H., Koseki, S., Matsunaga, N., Nguyen, K. A., Su, S., Windus, T. L., Dupuis, M., and Montgomery, J. A., Jr. (1993) General atomic and molecular electronic structure system. *J. Comput. Chem. 14*, 1347–1353.

(30) Wang, J., Cieplak, P., and Kollman, P. A. (2000) How well does a restrained electrostatic potential (RESP) model perform in calculating conformational energies of organic and biological molecules? *J. Comput. Chem. 21*, 1049–1074.

(31) Hornak, V., Abel, R., Okur, A., Strockbine, B., Roitberg, A., and Simmerling, C. (2006) Comparison of multiple Amber force fields and development of improved protein backbone parameters. *Proteins 65*, 712–725.

(32) Case, D. A., Cheatham, T. E., Darden, T., Gohlke, H., Luo, R., Merz, K. M., Onufriev, A., Simmerling, C., Wang, B., and Woods, R. J. (2005) The Amber biomolecular simulation programs. *J. Comput. Chem. 26*, 1668–1688.

(33) Case, D. A., Darden, T., Cheatham, T. E., Simmerling, C., Wang, J., Duke, R. E., Luo, R., Crowley, M., Walker, R. C., Zhang, W., Merz, K. M., Wang, B., Hayik, S., Roitberg, A., Seabra, G., Kolossvary, I., Wong, K. F., Paesani, F., Vanicek, J., Wu, X., Brozell, S. R., Steinbrecher, T., Gohlke, H., Yang, L., Tan, C., Mongan, J., Hornak, V., Cui, G., Mathews, D. H., Seetin, M. G., Sagui, C., Babin, V., and Kollman, P. A. (2008) *AMBER 10*, University of California, San Francisco.

(34) Jorgensen, W. L., Chandrasekhar, J., Madura, J. D., Impey, R. W., and Klein, M. L. (1983) Of simple potential functions for simulating liquid water. *J. Chem. Phys. 79*, 926–935.

(35) Darden, T., York, D., and Pedersen, L. (1993) Particle mesh Ewald: an N log(N) method for Ewald sums in large systems. *J. Chem. Phys. 98*, 10089–10092.

(36) Ryckaert, J. P., Ciccotti, G., and Berendsen, H. J. C. (1977) Numerical integration of the cartesian equations of motion of a system with constraints: molecular dynamics of n-alkanes. *J. Comput. Phys. 23*, 327–341.

(37) Pauly, T. A., Sulea, T., Ammirati, M., Sivaraman, J., Danley, D. E., Griffor, M. C., Kamath, A. V., Wang, I. K., Laird, E. R., Seddon, A. P., Ménard, R., Cygler, M., and Rath, V. L. (2003) Specificity determinants of human cathepsin s revealed by crystal structures of complexes. *Biochemistry 42*, 3203–3213.

(38) Schneck, J. L., Villa, J. P., McDevitt, P., McQueney, M. S., Thrall, S. H., and Meek, T. D. (2008) Chemical mechanism of a cysteine protease, cathepsin C, as revealed by integration of both steady-state and pre-steady-state solvent kinetic isotope effects. *Biochemistry 47*, 8697–8710.

(39) Ménard, R., Carrière, J., Laflamme, P., Plouffe, C., Khouri, H. E., Vernet, T., Tessier, D. C., Thomas, D. Y., and Storer, A. C. (1991) Contribution of the glutamine 19 side chain to transition-state stabilization in the oxyanion hole of papain. *Biochemistry 30*, 8924–8928.

(40) Dufour, E., Storer, A. C., and Ménard, R. (1995) Peptide aldehydes and nitriles as transition state analog inhibitors of cysteine proteases. *Biochemistry 34*, 9136–9143.

(41) Ménard, R., Plouffe, C., Laflamme, P., Vernet, T., Tessier, D. C., Thomas, D. Y., and Storer, A. C. (1995) Modification of the electrostatic environment is tolerated in the oxyanion hole of the cysteine protease papain. *Biochemistry 34*, 464–471.

(42) Vernet, T., Tessier, D. C., Chatellier, J., Plouffe, C., Lee, T. S., Thomas, D. Y., Storer, A. C., and Ménard, R. (1995) Structural and functional roles of asparagine 175 in the cysteine protease papain. *J. Biol. Chem. 270*, 16645–16652.

(43) Brömme, D., Bonneau, P. R., Purisima, E., Lachance, P., Hajnik, S., Thomas, D. Y., and Storer, A. C. (1996) Contribution to activity of histidine-aromatic, amide-aromatic, and aromatic-aromatic interactions in the extended catalytic site of cysteine proteinases. *Biochemistry 35*, 3970–3979.

(44) Messick, T. E., Russell, N. S., Iwata., A. J., Sarachan, K. L., Shiekhattar, R., Shanks, J. R., Reyes-Turcu, F. E., Wilkinson, K. D., and Marmorstein, R. (2008) Structural basis for ubiquitin recognition by the Otu1 ovarian tumor domain protein. *J. Biol. Chem. 283*, 11038–11049.

(45) Nanao, M. H., Tcherniuk, S. O., Chroboczek, J., Dideberg, O., Dessen, A., and Balakirev, M. Y. (2004) Crystal structure of human otubain 2. *EMBO Rep. 5*, 783–788.

(46) Lin, S. C., Chung, J. Y., Lamothe, B., Rajashankar, K., Lu, M., Lo, Y. C., Lam, A. Y., Darnay, B. G., and Wu, H. (2008) Molecular basis for the unique deubiquitinating activity of the NF-kB inhibitor A20. *J. Mol. Biol. 376*, 526–540.

(47) Case, A., and Stein, R. L. (2006) Mechanistic studies of ubiquitin C-terminal hydrolase L1. *Biochemistry 45*, 2443–2452.